JURNAL geografi

https://jurnal.unimed.ac.id/2012/index.php/geo/article/view/75454
https://doi.org/10.24114/jg.v18i2.75454 - (Vol 18, No 2 – 2026)
available at http://jurnal.unimed.ac.id/2012/index.php/geo
e-issn (2549-7057) & p-issn (2085-8167)

# Spatial and Temporal Patterns of Flickr Photographic Activity in Sleman's Temple Heritage Landscape

**Totok Wahyu Wibowo[1]*, Sigit Heru Murti Budi Santosa[1], Bowo Susilo[1], Taufik Hery Purwanto[1], Bayu Kurniawan[1]**

[1]Cartography and Remote Sensing Study Program, Department of Geographic Information Science, Faculty of Geography, Universitas Gadjah Mada, Indonesia

**ARTICLE INFO**

Article History:
Received: July 28, 2026
Revision: September 09, 2026
Accepted: September 11, 2026

Keywords:
Cultural Tourism;
Spatiotemporal Analysis;
Flickr;
Temple Heritage;
Indonesia.

Corresponding Author
E-mail: totok.wahyu@ugm.ac.id



**ABSTRACT**

Yogyakarta's Sleman Regency contains the Prambanan Temple Compounds, a UNESCO World Heritage Site, and a wider network of temple-related heritage locations whose spatiotemporal photographic patterns remain poorly characterized. This study analyzes 5,858 geotagged Flickr photographs recorded between 2005 and 2025 within analytical buffer zones for 13 temple-related heritage locations. Four complementary methods were used: quadrat density analysis, Getis-Ord Gi*-based Optimized Hot Spot Analysis (OHSA), Emerging Hot Spot Analysis (EHSA) through a Space-Time Cube, and HDBSCAN density-based clustering. Flickr photographic activity concentrates strongly in the Candi Prambanan analytical zone, which accounts for 82.14% of retained records. A Spearman rank-order comparison with 2023 official visitor statistics ($r_s = 0.979$, $p < 0.001$, $n = 9$) supports consistency in relative site prominence between the two data sources, though this result reflects rank-order agreement rather than validation of Flickr photographs as a direct measure of visitor volume. OHSA identifies a statistically significant hot spot at the 99% confidence level centered on the main temple precinct, with cold spot detection in peripheral areas sensitive to grid resolution. Within the Candi Prambanan analytical zone, EHSA classifies 372 locations, comprising 365 Oscillating Hot Spots and 7 Sporadic Hot Spots, indicating endpoint-dependent temporal fluctuation rather than sustained directional growth. HDBSCAN identifies 17 interpretable photographic clusters within the Candi Prambanan analytical zone corresponding to recognizable heritage features and visitor-use spaces, including the main temple core, eastern circulation corridors, the Archaeological Museum, Candi Lumbung, and the Ramayana Open Air Theater. The findings demonstrate that multi-year spatiotemporal analysis produces substantially different site characterizations than static hot spot mapping alone. The results support candidate prioritization for field-based visitor monitoring but should not be interpreted as direct evidence of visitor pressure, dwell time, or physical deterioration at any site.

## INTRODUCTION

Heritage tourism has grown substantially over the past two decades, driven by expanding interest in historical monuments, archaeological landscapes, and living cultural traditions (Kim et al., 2024; López-Guzmán et al., 2011). Growth brings economic and cultural opportunities, but it also concentrates spatial demands on heritage sites in ways that are difficult to manage without fine-grained data on where visitor attention actually falls (Adie et al., 2020). Official visitor statistics report aggregate arrivals at the site or administrative level, but they do not show which parts of a site attract the most photographic attention, whether concentration is shifting over time, or how attention distributes across secondary locations in the same landscape (Coimbra et al., 2025).

Multi-site heritage landscapes pose a specific version of this problem. Flagship attractions tend to absorb the majority of visitor attention, creating spatial imbalances where iconic sites dominate while surrounding heritage components remain peripheral (McKercher & Koh, 2017; Meng et al., 2025). In such settings, aggregate counts cannot reveal whether attention is concentrated around a single monument, dispersed across several components, or absent at secondary locations altogether. Understanding that structure requires data that operate at finer spatial resolution than official statistics alone can provide.

Geotagged photographs from social media platforms offer one route to this finer resolution. Flickr photographs frequently carry geographic coordinates and timestamps recorded at capture, making them usable as spatial event data for mapping where photographic attention concentrates within and across destinations (García-Palomares et al., 2015; Tenkanen et al., 2017). Previous studies have applied Flickr and other geotagged photo-sharing data to identify tourism hot spots, reconstruct visitor trajectories, and characterize destination image formation in settings ranging from historic city centers to archaeological landscapes (Domènech et al., 2020; Dong et al., 2023; Lee & Tsou, 2018; Payntar et al., 2021; Sedmak et al., 2023). Their value lies not in counting visitors directly, but in revealing where users choose to photograph and share.

Flickr data carry well-documented limitations. Platform demographics skew toward internationally connected, photography-oriented users; upload frequency varies widely across contributors; and platform activity declined substantially after the mid-2010s, so changes in annual photograph counts may reflect platform dynamics rather than changes in physical visitation (Fast, 2024; Leppämäki et al., 2025; Zhang & Zhu, 2018). Social media data more broadly are subject to demographic representation gaps, capturing only the perspectives of users who actively upload while leaving other visitor groups underrepresented (Ghermandi, 2022; Wilkins et al., 2021).

Flickr photographs measure photographic activity, not visitor counts, and should not be treated as a substitute for systematic monitoring (Haklay, 2013; Martins & Santos, 2024). Concentrations of photographs may indicate where visitors direct visual attention or where site components become prominent in digital representations, but they do not measure crowding, dwell time, or physical contact with monument surfaces. In this study, any discussion of management-relevant patterns is treated as a candidate signal requiring validation through field observation, direct counts, and conservation assessment.

Yogyakarta's Sleman Regency provides a productive setting for this kind of analysis. The regency contains the Prambanan Temple Compounds, a UNESCO World Heritage Site, and a wider network of Hindu-Buddhist temple heritage sites distributed across its eastern part. Candi Prambanan functions as the flagship attraction in this landscape. Surrounding sites, including Ratu Boko, Candi Ijo, Candi Sambisari, Candi Kalasan, Candi Sari, Candi Banyunibo, Candi Barong, and Candi Gebang, differ substantially in scale, accessibility, and tourism intensity while remaining embedded in the same cultural and administrative landscape. Candi Prambanan received 2,447,882 visitors in 2023; several surrounding temples recorded numbers orders of magnitude lower. This disparity makes Sleman a suitable case for examining how photographic attention distributes across a multi-site heritage landscape with a dominant flagship and multiple secondary locations.

Flickr-based tourism studies have concentrated largely in North America and Europe, and Southeast Asian heritage landscapes remain less represented in this literature (Ghermandi & Sinclair, 2019; Teles Da Mota & Pickering, 2020). Studies in Indonesia have focused mainly on individual destinations or specific tourism contexts, with fewer works examining temple heritage landscapes as connected spatial systems (Wibowo et al., 2019; Wicaksono et al., 2021). Studies that compare static hot spot detection, spatiotemporal classification, and density-based clustering within the same heritage landscape to assess how method choice shapes interpretation are also relatively uncommon (Bettaieb & Wakabayashi, 2023; Karayazi et al., 2022).

This study addresses those gaps through four complementary methods applied to 5,858 geotagged Flickr photographs located within analytical buffer zones for 13 temple-related heritage locations in Sleman Regency, covering records dated between 2005 and 2025. Quadrat density analysis maps the raw spatial distribution of photographs. OHSA, using the Getis-Ord Gi* statistic, identifies statistically significant spatial concentrations (Getis & Ord, 1992). EHSA, implemented through a Space-Time Cube, classifies the temporal behavior of hot spot patterns across annual time steps (Morckel & Durst, 2023; Purwanto et al., 2021). HDBSCAN clustering identifies intra-site photographic nodes within the Candi Prambanan analytical zone without requiring predefined cluster shapes or a fixed cluster count (Campello et al., 2013; McInnes et al., 2017). These four methods are applied in sequence and at complementary scales, from descriptive spatial mapping to statistical significance testing, temporal classification, and intra-site node delineation, allowing comparison of how each analytical lens characterizes photographic concentration in the same landscape.

The main contribution of this study is to show that Flickr-based heritage hot spots should not be interpreted from static spatial concentration alone. By combining static hot spot detection, spatiotemporal classification, and density-based intra-site clustering, the study demonstrates how photographic concentration can be separated from temporal stability and from direct claims about visitor pressure. Empirically, it provides a 21-year spatial and temporal characterization of Flickr photographic activity in Sleman's temple heritage landscape, a context underrepresented in the geotagged social media literature. The analysis is oriented toward identifying candidate areas for field-based visitor monitoring rather than drawing conclusions about physical conditions from photograph data alone.

Three research questions guide the analysis. First, where does Flickr photographic activity concentrate across the 13 heritage locations, and what spatial patterns emerge at site and intra-site levels? Second, how have photographic hot spot patterns evolved across annual time steps from 2005 to 2025? Third, which spatial nodes within the Candi Prambanan analytical zone show the highest photographic concentration, and what do those nodes suggest as candidate priorities for field-based monitoring?

## RESEARCH METHODS

### Study Area

Sleman Regency lies north of Yogyakarta City and borders Central Java Province. Its eastern part contains a dense network of Hindu-Buddhist temple sites dating from approximately the sixth to tenth centuries, distributed across a compact cultural landscape **(Figure 1)**. Three spatial units are relevant to understanding how the analysis is organized. The study corpus covers 13 temple-related heritage locations. Official visitor statistics are available only for selected managed destinations, reported in **Table 1**.

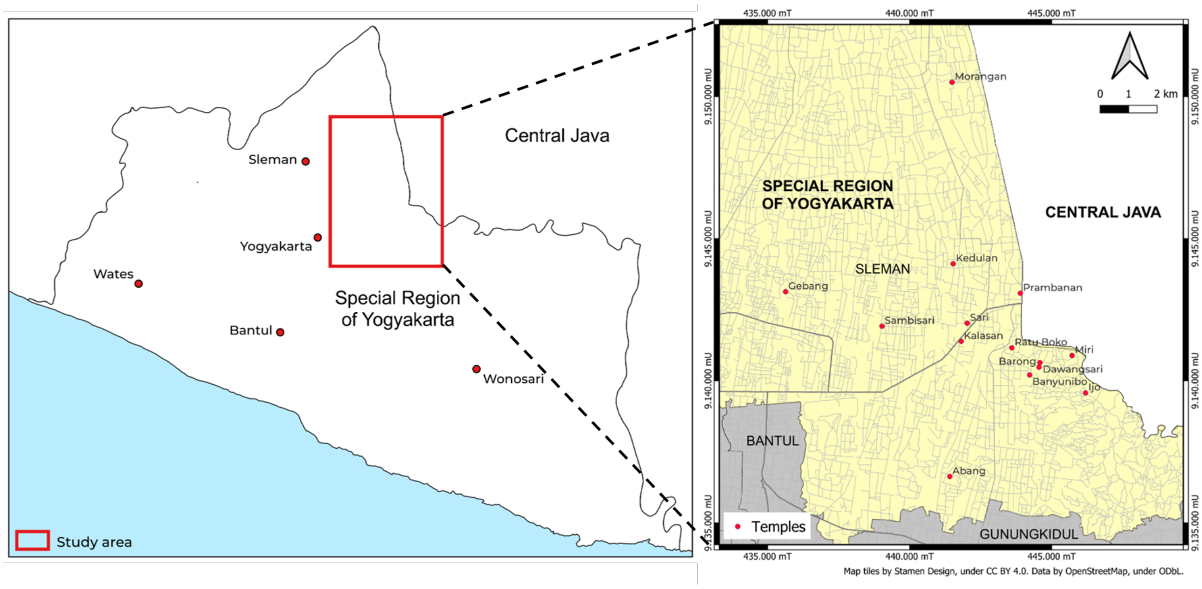


**Figure 1**. The location of temples in Sleman Regency (Source: Authors' analysis, 2026)

**Table 1**. Official visitor statistics and Flickr photograph counts for managed heritage destinations in Sleman Regency with available official records.

| No | Temple | Visitor 2021 | Visitor 2022 | Visitor 2023 | Number of Flickr Photos |
|---|---|---|---|---|---|
| 1. | Candi Prambanan | 262,107 | 1,772,780 | 2,447,882 | 4,812 |
| 2. | Ratu Boko Complex | 45,118 | 137,772 | 133,506 | 348 |
| 3. | Candi Ijo | 10,796 | 30,179 | 28,481 | 230 |
| 4. | Candi Sambisari | 15,114 | 35,312 | 29,073 | 161 |
| 5. | Candi Banyunibo | 665 | 1,221 | 621 | 38 |
| 6. | Candi Barong | 0 | 0 | 132 | 20 |
| 7. | Candi Sari | 0 | 1,410 | 2,052 | 70 |
| 8. | Candi Kalasan | 0 | 2,914 | 3,908 | 110 |
| 9. | Candi Gebang | 0 | 0 | 411 | 38 |

Source: Dinas Pariwisata Daerah Istimewa Yogyakarta (2024). Note: Flickr photograph counts cover the full 2005–2025 study period. Zero values in official visitor statistics are reported as published and may reflect unavailable or unreported records rather than confirmed absence of visitors. Table 1 reports managed heritage destinations for which official visitor statistics are available; Table 2 reports the analytical buffer zones used for spatial attribution of Flickr photographs. These two tables serve different analytical purposes and should not be interpreted as identical site inventories.

The main heritage attraction in the study area is the Prambanan Temple Compounds, which was inscribed as a UNESCO World Heritage Site in 1991 (UNESCO, 1991). The broader Prambanan visitor complex encompasses several heritage components and supporting visitor facilities, including Candi Prambanan, Candi Lumbung, Candi Bubrah, Candi Sewu, the Archaeological Museum, and the Ramayana Open Air Theater. Within this wider complex, the present study focuses on Candi Prambanan as the principal analytical location. Its central precinct comprises three principal temples dedicated to Shiva, Vishnu, and Brahma, together with three smaller temples situated to their east: Garuda, Nandi, and Hamsa. This focus allows the analysis to examine photographic activity around the main architectural ensemble while recognizing its position within the broader Prambanan heritage and visitor landscape.

Beyond the Candi Prambanan analytical zone, the corpus includes Ratu Boko Complex, Candi Ijo, Candi Sambisari, Candi Kalasan, Candi Sari, Candi Banyunibo, Candi Barong, Candi Gebang, Candi Abang, Candi Miri, Candi Kedulan, and Candi Morangan. These locations differ in scale, accessibility, visitor infrastructure, and tourism intensity. They are treated as components of a shared temple heritage landscape rather than isolated attractions.

**Data Acquisition**

This study adopts a spatial-first approach to dataset construction. Rather than filtering records based on the presence of heritage-related keywords in user-generated metadata, photographs were retained based on their geographic location within analytically defined buffer zones (Domènech et al., 2020; Tenkanen et al., 2017). This decision reflects the nature of Flickr metadata: user-generated titles and tags are frequently incomplete, generic, or absent, and many records carry file-system defaults or broad activity descriptions that do not identify the photographed subject (Sigurbjörnsson & Van Zwol, 2008). Because the analytical methods used here rely on coordinates and timestamps rather than image content or semantic metadata, spatial location is the primary criterion for inclusion. The retained photographs are therefore interpreted as geotagged Flickr photographic activity within temple-related analytical zones, not as a visually verified corpus of photographs depicting temple structures (Mancini et al., 2018).

Flickr photograph metadata were retrieved through the *flickr.photos.search* API endpoint on 2 May 2026. The search bounding box covered Yogyakarta and surrounding areas (109.934°E to 110.965°E, 8.325°S to 7.435°S), using a broader extent than the study area to avoid excluding photographs near administrative boundaries or site edges. The initial retrieval returned 105,210 photographs. Of these, 5,858 fell within the 13 defined analytical buffer zones and were retained for analysis. Buffer zones around each heritage location defined the operational spatial units for photograph attribution and density analysis. A uniform buffer radius was not applied. The study area contains both compact single temples and large heritage complexes, and several sites are located within relatively close spatial settings where equal radii would either overextend small sites or create ambiguous spatial attribution of photographs to nearby heritage components.

Radii were assigned through expert-guided operational judgement based on the physical scale of each site, the compactness of its visitor-use area, expected photographic catchment, surrounding access space, and proximity to other heritage components. Because analytical zones differ in area by up to two orders of magnitude, raw photograph counts are zone totals rather than comparable indicators of photographic intensity. **Table 2** reports buffer radius, zone area, total photographs, and photographs per hectare for each site.

The earliest retained photograph dates to 3 February 2005 and the latest to 19 December 2025. The 2025 records therefore cover nearly the full calendar year and are retained as the final annual time step. The 5,858 photographs were contributed by 606 unique Flickr users, with individual contributions ranging from 1 to 253 photographs (mean 9.68, median 3). Several prolific contributors may therefore influence local photograph densities. The unit of analysis throughout is the photograph, not the visitor or visit.

Flickr assigns each photograph a positional accuracy code from 1 (world level) to 16 (street level) (Hollenstein & Purves, 2010). Retained records span levels 9 to 16, but 86.77% carry level 16 and 96.19% fall within levels 14 to 16 **(Table 3)**. Accuracy codes are categorical localization levels rather than metric error estimates. The 10 m analytical grid functions as a visualization and aggregation framework, not as a claim of positional precision at that scale.

Candi Abang produced only two retained photographs after spatial attribution. It is retained in the dataset for corpus completeness but is not interpreted at the site level because two observations cannot support a meaningful characterization of its spatial distribution.

Flickr metadata were obtained through the API in accordance with its Terms of Use (Flickr, 2024). No individual photographs are reproduced. User identifiers were used only to calculate aggregate contributor statistics, and all results appear in aggregated spatial or statistical form.

**Table 2**. Analytical buffer zones used for spatial attribution of Flickr photographs in Sleman Regency.

| No | Site / Analytical Unit | Buffer Radius (m) | Zone Area (ha) | Flickr Photos | Photos/ha | Buffer Rationale |
|---|---|---|---|---|---|---|
| 1 | Candi Abang | 20 | 0.13 | 2 | 15.4 | Conservative point-centered buffer used to capture immediate site-related photographic records and limit over-attribution |
| 2 | Candi Barong | 20 | 0.13 | 20 | 153.8 | Conservative point-centered buffer used to capture immediate site-related photographic records and limit over-attribution |
| 3 | Candi Miri | 50 | 0.79 | 5 | 6.3 | Small isolated site with minimal surrounding visitor infrastructure |
| 4 | Candi Ijo | 80 | 2.01 | 230 | 114.4 | Moderate site with hillside approach, western viewing area, and dispersed photographic activity |
| 5 | Candi Kedulan | 100 | 3.14 | 10 | 3.2 | Moderate single-site setting; buffer captures immediate grounds and likely photographic viewpoints |
| 6 | Candi Kalasan | 100 | 3.14 | 110 | 35 | Moderate single-site setting; buffer captures immediate grounds and likely photographic viewpoints |
| 7 | Candi Banyunibo | 100 | 3.14 | 38 | 12.1 | Moderate single-site setting; buffer captures immediate grounds and likely photographic viewpoints |
| 8 | Candi Morangan | 150 | 7.07 | 14 | 2 | Wider catchment assigned to small site with surrounding open space and potential off-structure photographic viewpoints |
| 9 | Candi Gebang | 150 | 7.07 | 38 | 5.4 | Wider catchment for surrounding access and open-space photographic activity |
| 10 | Candi Sari | 150 | 7.07 | 70 | 9.9 | Wider catchment for surrounding access and open-space photographic activity |
| 11 | Candi Sambisari | 200 | 12.57 | 161 | 12.8 | Below-ground excavated structure with surrounding visitor platform, grounds, and access paths |
| 12 | Ratu Boko Complex | 250 | 19.63 | 348 | 17.7 | Large hilltop heritage complex with dispersed |

| | | | | | | |
|---|---|---|---|---|---|---|
| | | | | | | architectural components across multiple terraces |
| 13 | Candi Prambanan analytical zone | 500 | 78.54 | 4,812 | 61.3 | Large heritage complex with multiple components, visitor facilities, and extensive circulation area |
| **Total** | | | | **5,858** | | |

Note: Buffer radii are operational analytical choices based on site scale, expected photographic catchment, visitor-use space, and proximity to other heritage components. They do not represent official heritage boundaries. Raw counts should be interpreted alongside photographs per hectare. Different buffer choices would affect retained photograph counts and site-level comparisons; this is acknowledged as a methodological limitation.

**Table 3**. Distribution of Flickr API positional accuracy codes in the retained dataset.

| Accuracy Level | Photographs (n) | Percentage (%) |
|---|---|---|
| 9 | 18 | 0.31 |
| 10 | 44 | 0.75 |
| 11 | 13 | 0.22 |
| 12 | 89 | 1.52 |
| 13 | 59 | 1.01 |
| 14 | 275 | 4.70 |
| 15 | 277 | 4.73 |
| 16 | 5,083 | 86.77 |
| **Total** | **5,858** | **100.00** |

Note: Flickr accuracy codes are categorical localization levels from 1 (world) to 16 (street), not metric error estimates.

**Analytical Framework**

Four complementary methods characterize Flickr photographic activity at different spatial and temporal scales, supplemented by Spearman rank-order correlation to evaluate consistency with official visitor statistics. Quadrat density analysis maps raw photograph concentration. OHSA identifies locations where counts are statistically higher or lower than expected under spatial randomness. EHSA classifies the temporal behavior of hot spot and cold spot patterns using a Space-Time Cube and the Mann-Kendall trend test (ESRI, 2021; Morckel & Durst, 2023). HDBSCAN clustering identifies dense intra-site photographic nodes within the Candi Prambanan analytical zone without requiring a predefined cluster count (Campello et al., 2013; McInnes et al., 2017). Finally, Spearman rank correlation assesses the monotonic alignment between retained Flickr photograph counts and official visitor statistics across managed sites.

The analytical workflow applies these methods in sequence: quadrat density maps spatial distribution descriptively, OHSA tests for statistical significance of spatial concentrations, EHSA evaluates whether hot spot patterns persist or fluctuate over time, HDBSCAN isolates micro-scale photographic nodes, and Spearman rank correlation assesses external dataset alignment. Comparing outputs across these methods enables an assessment of how analytical scale and method choice influence heritage-site characterization.

**Quadrat Density Analysis**

Quadrat density analysis was used to map the spatial concentration of Flickr photographs across the study area. A 10 m grid was selected as the analytical unit because it approximates the spatial scale of recognizable heritage features such as temple platforms, entrance corridors, and viewing areas, allowing photographic concentration to be examined at a level of detail meaningful for site-level interpretation. The 10 m resolution is not a claim that all retained photographs are accurate to that scale; it serves as an aggregation and visualization framework consistent with the positional accuracy distribution reported in **Table 3**.

The number of photographs falling within each grid cell was counted, and cells containing no photographs were excluded from visualization. To visualize the resulting density surface, cell counts were classified using Natural Breaks (Jenks, 1967). This classification method groups values by minimizing within-class variation and maximizing separation between classes, making it suitable for highlighting spatial contrasts in photographic concentration where the data distribution is uneven, as is the case in a dataset dominated by one analytical zone.

**Optimized Hot Spot Analysis (OHSA)**

OHSA was applied to the gridded photograph counts for all 13 temple-related locations using the Getis-Ord Gi* statistic in ArcGIS Desktop 10.8. The statistic measures whether the local concentration of photograph counts around each grid cell is significantly higher or lower than expected under spatial randomness, using a fixed distance band to define the neighborhood. Cells outside the specified threshold do not contribute to the local statistic.

The analysis was conducted at three grid sizes: 10 m, 20 m, and 30 m. The 10 m grid serves as the primary analytical scale, consistent with the quadrat density analysis; the 20 m and 30 m grids were included to assess sensitivity to spatial resolution.

For each grid size, the fixed distance threshold was determined using Incremental Spatial Autocorrelation applied to the combined analytical grid across the study area. Where ISA yielded a statistically significant peak, the corresponding distance was used as the main threshold. The 30 m grid did not produce a statistically significant ISA peak; therefore, the selected distance was retained as an exploratory reference threshold rather than interpreted as an optimal distance.

OHSA was subsequently repeated using distance bands 20% below and 20% above each main or reference threshold. The combination of three grid sizes and three distance settings produced nine analytical configurations. For each configuration, grid cells were classified as statistically significant hot spots, cold spots, or non-significant at the 90%, 95%, and 99% confidence levels. False Discovery Rate correction was applied throughout to reduce the risk of spurious local significance under multiple spatial tests (Caldas de Castro & Singer, 2006). Comparing classifications across configurations was used to evaluate whether local hot spot patterns were stable across analytical choices or sensitive to grid resolution and neighborhood distance.

**Emerging Hot Spot Analysis (EHSA)**

EHSA was applied to examine how Flickr photographic activity changed across annual time steps from 2005 to 2025. For each of the 13 temple-related locations, a Space-Time Cube was constructed in ArcGIS Desktop 10.8 by aggregating photograph counts into 10 m spatial bins at annual time steps. Annual aggregation was selected because the Flickr records are too sparse to support consistent interpretation at finer temporal intervals.

EHSA applies the Getis-Ord Gi* statistic to each space-time neighborhood and then uses the Mann-Kendall trend test to classify the temporal behavior of statistically significant hot spot and cold spot patterns. The classification framework includes new, consecutive, intensifying, persistent, diminishing, sporadic, oscillating, and historical patterns in both hot spot and cold spot variants (ESRI, 2021; Morckel & Durst, 2023).

A spatial neighborhood distance of 187.28 m and a one-year temporal interval were applied consistently across the analysis. Before interpreting EHSA classifications, the Space-Time Cube outputs were examined for the number of analyzed locations, annual time steps, total space-time bins, non-zero bins, neighborhood distance, and temporal interval. These diagnostics inform how the resulting classifications should be read in light of spatial and temporal data sparsity. The absence of a classified EHSA pattern indicates that the available Flickr records did not produce a statistically classifiable spatiotemporal pattern under the selected spatial and temporal settings. It should not be interpreted as evidence of temporal stability or absence of photographic activity.

**HDBSCAN Clustering**

HDBSCAN was applied to the 4,812 photographs within the Candi Prambanan analytical zone to identify dense intra-site photographic nodes. The method detects clusters of variable density and irregular shape, requires no predefined cluster count, and assigns low-density observations to noise rather than forcing them into clusters. These characteristics suit heritage settings where photographs may cluster around monuments, entrances, pathways, viewpoints, performance spaces, and visitor facilities.

Clustering was run in GeoDa 1.22 using projected UTM Zone 49S coordinates (EPSG:32749), standardized coordinates, Euclidean distance, and the Excess of Mass extraction method. Parameter sensitivity was evaluated across eight combinations of minimum cluster size and minimum points: 10/3, 10/5, 20/5, 30/10, 50/10, 50/15, 60/10, and 60/15.

For each configuration, the number of clusters, clustered observations, noise observations, and noise ratio were recorded. Silhouette Score and Davies-Bouldin Index were calculated in Python using the cluster labels returned by GeoDa after excluding noise observations. These metrics served as supplementary diagnostics rather than absolute selection criteria, because configurations with many small clusters can produce favorable metric values while remaining difficult to map to recognizable heritage features.

The final configuration was determined in the Results section by considering cluster parsimony, noise proportion, diagnostic metrics, and spatial interpretability against recognizable heritage and visitor-use spaces. For the selected configuration, per-cluster summaries were produced covering photograph counts, unique Flickr user counts, centroid locations, dominant location, and functional category.

**Model Validation and Robustness**

The spatial data-construction workflow is traceable: 105,210 photographs were retrieved through the Flickr API, and 5,858 fell within the defined analytical buffer zones. Because the final dataset is spatially defined rather than semantically filtered, some retained photographs may not depict heritage structures directly. This is why results are interpreted as photographic activity within analytical zones throughout, not as a visually verified set of temple-structure photographs.

Positional accuracy was assessed using Flickr accuracy codes, which represent categorical localization levels rather than metric error estimates. The 10 m grid therefore functions as an aggregation and visualization framework, not a precision claim. The distribution of accuracy codes is reported in **Table 3**.

User-contribution bias was assessed at two levels: across the full dataset, where the number of unique users and the spread of individual contributions were calculated; and at the cluster level, where unique user counts were recorded for each HDBSCAN cluster after configuration selection. Clusters with high photograph counts but few contributing users are interpreted with caution, as they may reflect repeated uploads from a small number of individuals rather than broadly shared photographic attention.

Buffer radius choices are treated as a transparent operational limitation. Because analytical zones differ substantially in area, raw photograph counts are reported alongside area-adjusted density values in **Table 2**. Different radius choices would affect photograph volumes per site, and this variability is carried through the site-level interpretation.

OHSA sensitivity was assessed for all 13 temple-related locations across nine configurations combining three grid sizes (10 m, 20 m, and 30 m) with three distance settings. This comparison tested whether hot spot and cold spot classifications changed with spatial resolution and neighborhood distance.

EHSA temporal robustness was assessed through Space-Time Cube diagnostics. The number and temporal distribution of non-zero bins, neighborhood distance, and temporal interval were examined before interpreting the hot spot categories. These diagnostics were used to interpret the classifications in light of data sparsity, platform decline, and temporal gaps.

HDBSCAN robustness was assessed through the parameter sweep, comparing configurations on cluster count, clustered and noise observations, noise ratio, Silhouette Score, Davies-Bouldin Index, and spatial interpretability. Photographs classified as noise did not meet the density criteria under a given configuration and are not interpreted as evidence of any spatial pattern.

The Spearman comparison used 2023 official visitor statistics and total retained Flickr photographs for the nine managed heritage destinations with available records. Sites without official visitor statistics and intra-complex sub-zones such as Candi Lumbung were excluded. Zero values in earlier official statistics may reflect unavailable or unreported records rather than confirmed absence of visitors.

## RESULTS AND DISCUSSION

### Rank-Order Consistency of Flickr Photographic Activity

A Spearman rank-order comparison between total retained Flickr photograph counts and 2023 official visitor statistics across the nine managed heritage destinations yielded $r_s = 0.979$ ($p < 0.001$, $n = 9$), indicating strong consistency in relative site prominence between the two data sources. Sites with higher official visitor counts in 2023 generally produced more Flickr photographs over the 2005 to 2025 study period. **Table 1** shows that Candi Prambanan recorded the highest official visitor count in 2023, with 2,447,882 arrivals, and also contributed the largest number of retained Flickr photographs.

This result should be interpreted as rank-order consistency rather than validation of Flickr photographs as a direct measure of visitor volume. Official statistics represent annual visitor arrivals, whereas Flickr records reflect volunteered photographic uploads accumulated over a longer period and shaped by platform use, user participation, and photographic practices. The two data sources therefore offer complementary but non-equivalent views of heritage-site prominence (Martins & Santos, 2024; Tenkanen et al., 2017; Zhang & Zhu, 2018).

### Spatial Distribution of Photographic Activity

The retained Flickr dataset is spatially uneven. **Figure 2a** shows the full distribution of retained photographs across the study corpus; **Figure 2b** shows the Candi Prambanan analytical zone in detail. The Candi Prambanan analytical zone accounts for 4,812 of the 5,858 retained photographs (82.14%), a concentration broadly consistent with its role as Sleman's flagship heritage attraction, although Flickr photographs should not be interpreted as proportional to official visitor counts.

Raw photograph counts do not account for differences in analytical zone size. **Table 2** shows that the Candi Prambanan analytical zone, with its 500 m buffer, produces approximately 61 photographs per hectare, while Candi Ijo produces approximately 114 photographs per hectare within its smaller 80 m buffer. Absolute counts reflect flagship dominance; area-adjusted density captures localized photographic intensity at smaller sites.

**Figure 3** shows quadrat density at the Candi Prambanan analytical zone, Ratu Boko Complex, and Candi Ijo. At the Candi Prambanan analytical zone, high-density cells concentrate around the central temple precinct and extend eastward along the main visitor approach, with a secondary concentration near the Ramayana Open Air Theater. The zone combines monumental architecture, visitor circulation spaces, performance facilities, and secondary heritage components, consistent with studies showing that geotagged photographs cluster around prominent landmarks, pathways, and supporting attractions rather than administrative boundaries (García-Palomares et al., 2015; Urry & Larsen, 2011).

At Ratu Boko, photographs are distributed across the entrance area, ceremonial terraces, and southeastern architectural components. The elevated position and panoramic sightline toward Prambanan plausibly contribute to this dispersed pattern, consistent with findings on scenic viewpoints and visitor photography elsewhere (Lew & McKercher, 2006). At Candi Ijo, photographs concentrate around the main temple structure and western approach. Its high photographs-per-hectare value reflects localized photographic intensity within a small analytical zone. The site's proximity to Tebing Breksi may contextualize its photographic visibility, though inter-attraction movement is not measured here.

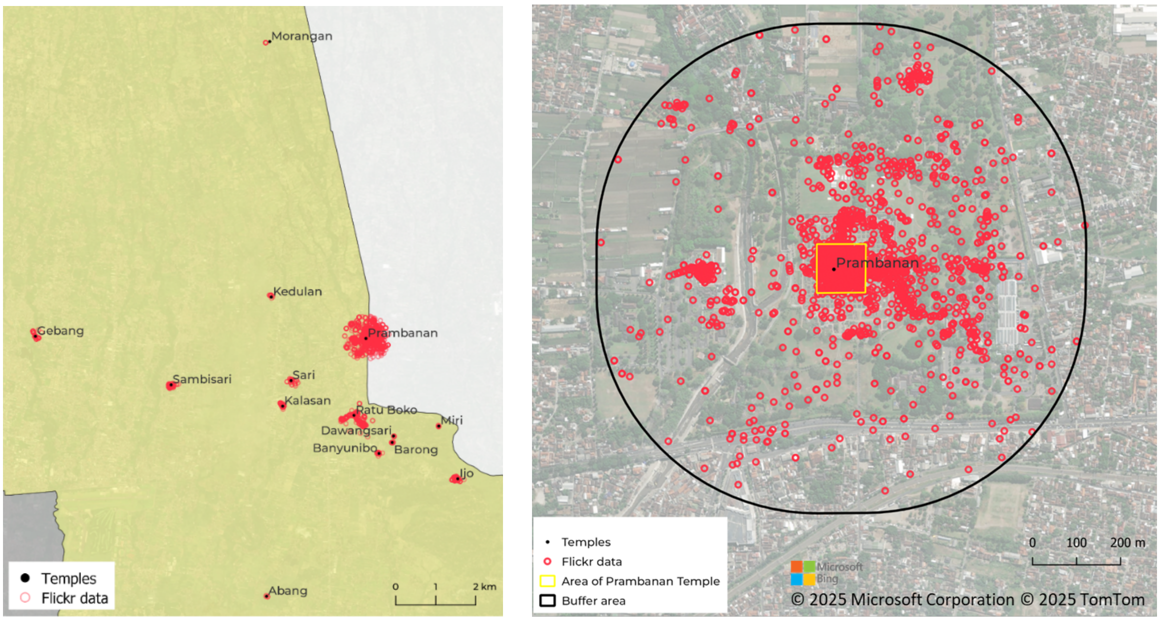


(a) (b)

**Figure 2.** Distribution of retained Flickr photographs after spatial attribution to analytical buffer zones: (a) full study corpus and (b) closer view of the Candi Prambanan analytical zone (Source: Authors' analysis, 2026)

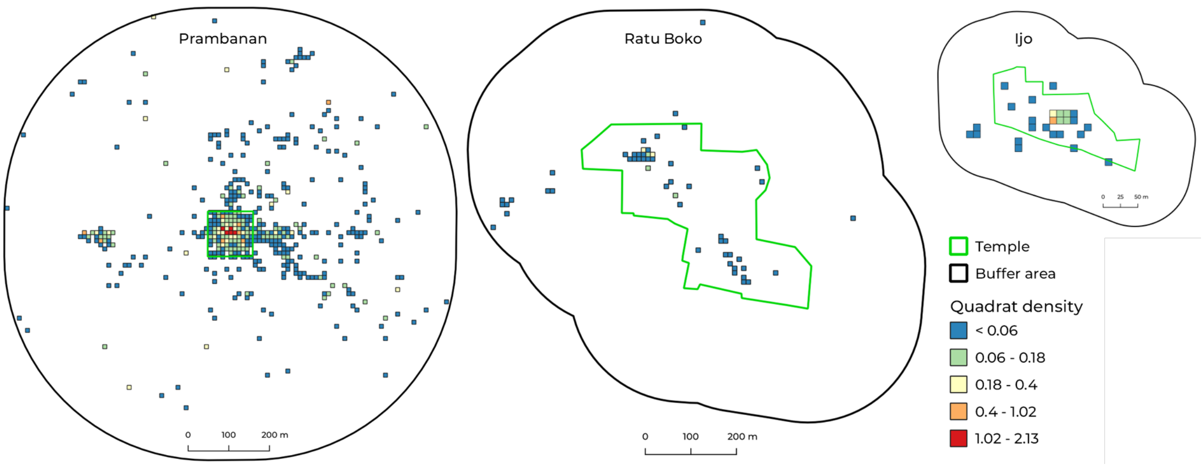


**Figure 3**. Quadrat density in the Candi Prambanan analytical zone, Ratu Boko Complex, and Candi Ijo (Source: Authors' analysis, 2026)

Remaining sites, including Candi Sambisari, Candi Kalasan, Candi Sari, Candi Banyunibo, Candi Barong, Candi Gebang, Candi Miri, Candi Kedulan, and Candi Morangan, contribute sparse records. Their limited representation reflects a known property of volunteered geographic information: data density follows platform use, destination visibility, and user interest rather than heritage significance or management need (Haklay, 2013; Zhang & Zhu, 2018).

**Hot Spot Identification and Statistical Significance**

OHSA was applied to all 13 temple-related locations. Statistically significant local classifications emerged only within the Candi Prambanan analytical zone and Ratu Boko Complex: Prambanan produced both hot spot and cold spot classifications, whereas Ratu Boko produced only cold spots. At the remaining locations, the available photograph counts and within-site spatial distributions did not produce statistically significant local classifications under the tested configurations. The non-significant results are interpreted in relation to the lower density and more limited spatial variation of the available Flickr records, rather than as evidence that these sites lack photographic, heritage, or management relevance.

**Figure 4** presents the statistically significant OHSA results for the Candi Prambanan analytical zone and Ratu Boko Complex. Incremental Spatial Autocorrelation identified the strongest statistically significant clustering at 350.51 m for the 10 m grid ($z = 3.116$, $p = 0.0018$) and at 369.11 m for the 20 m grid ($z = 2.014$, $p = 0.0441$). The 30 m grid produced no statistically significant ISA peak; 384.50 m was retained as an exploratory reference distance. These values served as the main or reference distance bands and were tested at 20% below and 20% above the selected distances, producing nine OHSA configurations. **Table 4** summarizes the resulting hot spot, cold spot, and non-significant classifications across the study area. Because statistically significant classifications emerged only within the Candi Prambanan analytical zone and Ratu Boko Complex, the spatial interpretation focuses on these two locations.

At the Candi Prambanan analytical zone, a 99% confidence hot spot centers on the main temple precinct and extends toward adjacent visitor-use spaces. The Ramayana Open Air Theater falls within the broader hot spot zone, indicating that photographic activity organizes around multiple cultural and visitor-use nodes rather than the central monument alone (Leask, 2016; Timothy & Boyd, 2003).

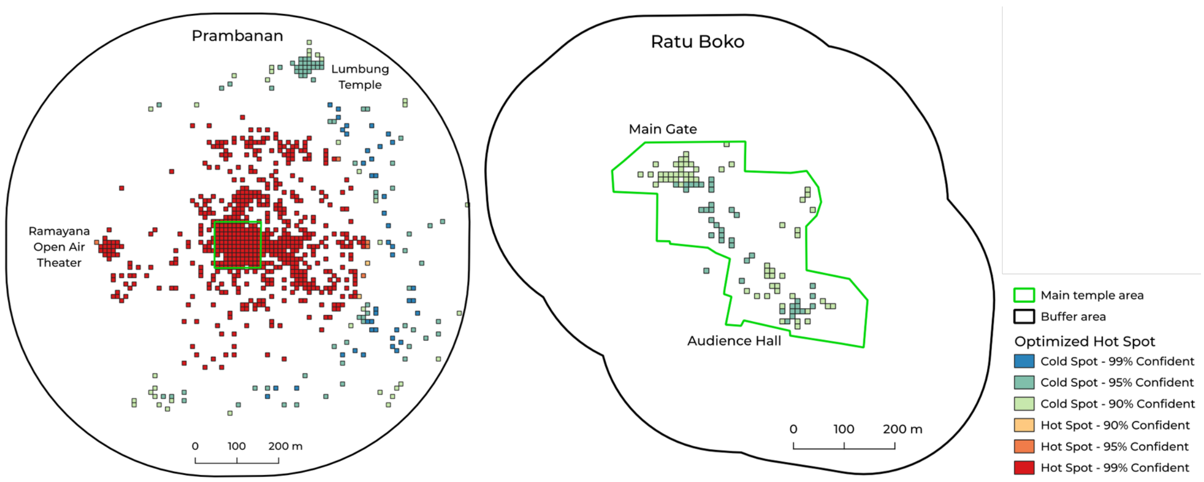


**Figure 4**. Optimized Hot Spot Analysis results for the Candi Prambanan analytical zone and Ratu Boko Complex using a 10 m grid (Source: Authors' analysis, 2026)

**Table 4**. OHSA sensitivity analysis across the study area using alternative grid sizes and fixed distance-band settings.

| Grid Size | Distance Band | HS 99% | HS 95% | HS 90% | NS | CS 90% | CS 95% | CS 99% | Total HS | Total CS |
|---|---|---|---|---|---|---|---|---|---|---|
| 10 m | 280.41 m (−20%) | 538 | 6 | 4 | 495 | 93 | 87 | 30 | 548 | 210 |
| 10 m | 350.51 m (main) | 655 | 3 | 3 | 355 | 95 | 104 | 38 | 661 | 237 |
| 10 m | 420.61 m (+20%) | 730 | 39 | 1 | 255 | 49 | 143 | 36 | 770 | 228 |
| 20 m | 295.28 m (−20%) | 252 | 9 | 2 | 520 | 0 | 0 | 0 | 263 | 0 |
| 20 m | 369.11 m (main) | 334 | 5 | 3 | 436 | 5 | 0 | 0 | 342 | 5 |
| 20 m | 442.93 m (+20%) | 369 | 51 | 3 | 330 | 30 | 0 | 0 | 423 | 30 |
| 30 m | 307.60 m (−20%) | 189 | 103 | 7 | 272 | 0 | 0 | 0 | 299 | 0 |
| 30 m | 384.50 m (ref.) | 69 | 162 | 131 | 209 | 0 | 0 | 0 | 362 | 0 |
| 30 m | 461.40 m (+20%) | 19 | 74 | 225 | 253 | 0 | 0 | 0 | 318 | 0 |

Note: HS = Hot Spot; CS = Cold Spot; NS = Not Significant. Distance thresholds were derived from Incremental Spatial Autocorrelation applied to the combined analytical grid across the study area: 350.51 m for the 10 m grid ($z = 3.116$, $p = 0.0018$), 369.11 m for the 20 m grid ($z = 2.014$, $p = 0.0441$), and 384.50 m as an exploratory reference threshold for the 30 m grid because no statistically significant ISA peak was detected. Sensitivity was evaluated at 20% below and 20% above each main or reference threshold. The table summarizes classifications for 1,253 cells at the 10 m grid, 783 cells at the 20 m grid, and 571 cells at the 30 m grid across the study area.

Cold spot classifications reveal further internal differentiation within the zone. At the 10 m grid, 95% confidence cold spots appear around the Candi Lumbung sub-zone, while 99% confidence cold spots concentrate in the southeastern part of the zone, corresponding to the parking and ticketing area. Both patterns reflect relative photographic concentration, not absence of visitors or management relevance. In OHSA, a cold spot indicates that Flickr photographic activity at a location is significantly lower than in its surrounding spatial neighborhood, which here is dominated by the highly photographed Shiva-Vishnu-Brahma core.

The Candi Lumbung result is analytically notable. A secondary heritage component within the broader analytical zone can remain photographically marginal in static hot spot analysis while still attracting multi-user photographic activity, a distinction that only becomes visible when OHSA is read alongside the HDBSCAN clusters discussed below. The southeastern cold spot may partly reflect site function because the parking and ticketing areas primarily serve circulation and access rather than functioning as major photographic subjects. **Table 4** shows that both peripheral cold spot patterns are sensitive to grid resolution, visible at 10 m but weakening or disappearing at coarser configurations, while the main hot spot around the temple core remains consistent across all nine tested configurations.

At Ratu Boko, **Figure 4** shows a weaker statistical structure. Across the tested configurations, the analysis produced only cold spots at the 90% and 95% confidence levels and no statistically significant hot spot. The 95% confidence cold spot falls around the inner main gate area, including the five-gate formation, a visually prominent feature well suited for silhouette photography. That a visually prominent feature reads as a cold spot reflects a distinction worth noting: visual prominence does not guarantee statistical concentration. Photographs at Ratu Boko are distributed across a large, terraced complex with multiple architectural components and viewpoints, and this dispersal reduces the local spatial contrast needed to form a statistically significant hot spot. The result is better read as dispersed photographic activity that did not generate a compact statistical concentration than as evidence of low photographic relevance, consistent with the sensitivity of local hot spot statistics to data density and spatial support in unevenly distributed volunteered geographic data (Al-Saad et al., 2023).

Descriptive density mapping and complementary qualitative approaches remain more appropriate for interpreting the remaining sparsely represented sites (Widjanarko et al., 2023).

### Spatiotemporal Dynamics and Emerging Patterns

EHSA was applied to the annual space-time grids for all 13 temple-related locations. Statistically classified temporal hot spot patterns emerged only within the Candi Prambanan analytical zone. The remaining locations did not produce statistically significant EHSA pattern classifications under the selected 10 m spatial resolution and annual temporal interval.

**Figure 5** shows the annual distribution of retained Flickr photographs in the Candi Prambanan analytical zone from 2005 to 2025. Counts peak around 2015, decline gradually afterward, drop sharply during 2020 to 2021, and recover partially from 2022 onward. Official statistics show strong recovery in 2023, while Flickr activity for that year remains comparatively low. This divergence is interpreted in relation to two broader contextual factors: the platform-wide decline in Flickr uploads after the mid-2010s and COVID-19 travel restrictions during 2020–2021, particularly given Flickr's internationally connected user base (Leppämäki et al., 2025; Mariani & Baggio, 2022). The annual Flickr series should therefore be interpreted as platform-mediated photographic activity rather than as a direct representation of physical visitation.

**Figure 6** shows the EHSA results for the Candi Prambanan analytical zone. Its Space-Time Cube spans 1,272 analyzed locations and 21 annual time steps, producing 26,712 space-time bins, of which 2,175 (8.14%) contain at least one photograph. Of 372 locations with statistically significant temporal hot spot patterns, 365 are classified as Oscillating Hot Spots and 7 as Sporadic Hot Spots. No locations carry new, consecutive, intensifying, persistent, diminishing, historical, or cold spot classifications. Both reported categories require statistically significant hot spot status in the final time step and are distinguished by their preceding temporal histories.

This endpoint dependency is important because the 2025 time step contains only 94 photographs, representing 1.95% of the 4,812 records in the Candi Prambanan analytical zone. This is the second-lowest annual count in the 21-year series and substantially lower than the peak of approximately 670 photographs in 2015. The reported distribution of Oscillating and Sporadic Hot Spots is therefore conditional on the selected 2005–2025 temporal window. Ending the series in a different year could change which locations satisfy the final-interval significance criterion and produce a different distribution of EHSA categories.

The emergence of statistically classified EHSA patterns only within the Candi Prambanan analytical zone reflects the uneven spatiotemporal distribution of Flickr records across the study corpus. Prambanan contains the largest number of photographs and the broadest spatial and annual coverage, although its cube remains sparse, with only 8.14% of the analyzed bins containing at least one photograph. The substantially smaller and more temporally discontinuous records at the other sites did not produce statistically significant EHSA pattern classifications under the selected spatial and temporal settings.

The absence of classified EHSA patterns at the remaining sites should not be interpreted as evidence of temporal stability or absence of photographic activity. It indicates that the available records did not form statistically classifiable spatiotemporal patterns at the 10 m spatial resolution and annual temporal interval used in this study. Detailed EHSA interpretation is therefore limited to the Candi Prambanan analytical zone.

Subject to this endpoint sensitivity, the predominance of Oscillating Hot Spots suggests that the strong spatial prominence identified by static hot spot analysis was not temporally uniform across the 21-year study period. The main temple area repeatedly appears as photographically prominent, but the strength of this prominence varies across annual time steps, consistent with the annual series in **Figure 5**. Studies using a shorter temporal window or a different endpoint could produce different EHSA classifications and might not capture this longer-term variation (Bettaieb & Wakabayashi, 2023; Morckel & Durst, 2023).

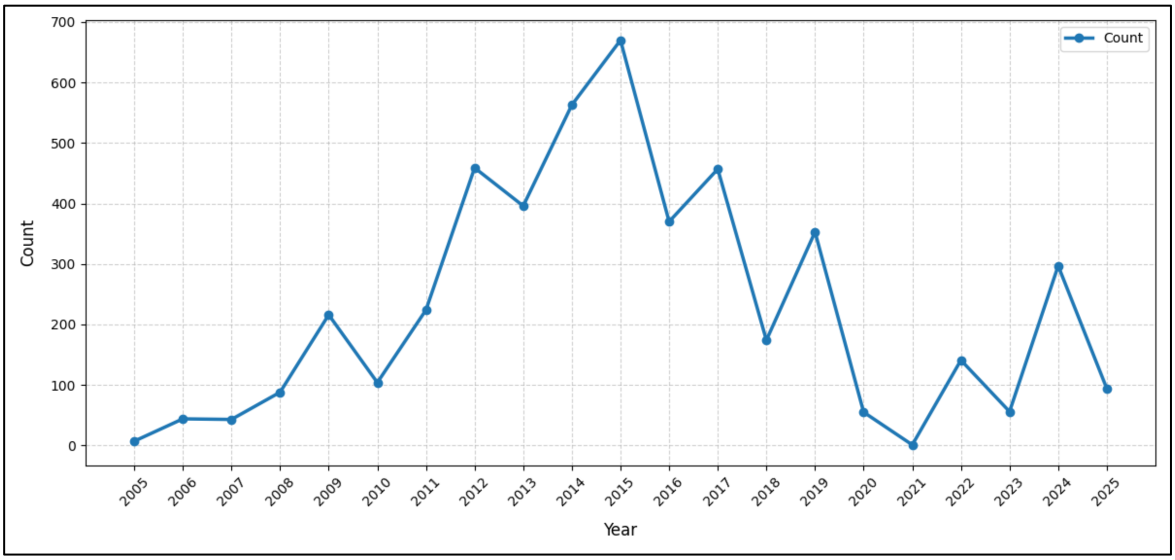


**Figure 5**. Annual number of retained Flickr photographs in the Candi Prambanan analytical zone, 2005–2025 (Source: Authors' analysis, 2026)

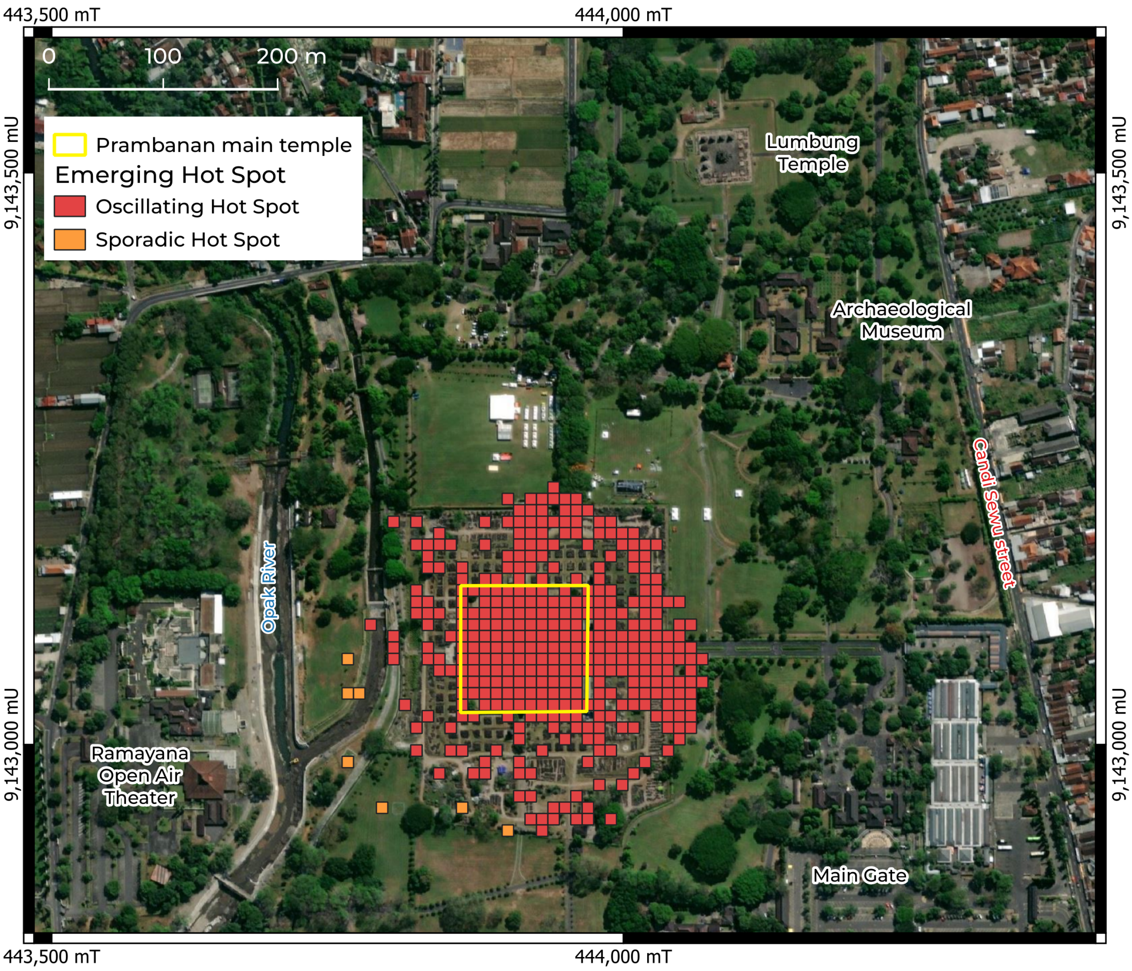


**Figure 6**. Emerging Hot Spot Analysis results for the Candi Prambanan analytical zone (Source: Authors' analysis, 2026)

**Intra-Site Photographic Nodes**

Parameter selection for HDBSCAN followed a systematic sweep across eight combinations of minimum cluster size and minimum points, with Silhouette Score and Davies-Bouldin Index calculated for each configuration on clustered observations only **(Table 5).**

The parameter sweep shows a trade-off between cluster fragmentation, noise proportion, and interpretability. The 10/5 configuration produced the highest Silhouette Score (0.722) but generated 143 clusters, while the 50/15 configuration produced the lowest DBI (0.356) with 22 clusters. The 60/15 configuration was selected because it produced the most parsimonious spatial structure, with 17 clusters that map to recognizable heritage and visitor-use spaces within the Candi Prambanan analytical zone.

HDBSCAN clustering of the 4,812 photographs identifies 17 spatial clusters comprising 2,151 clustered photographs, with 2,661 observations classified as noise (55.3%). The spatial distribution of these clusters is shown in **Figure 7**, and per-cluster statistics including photograph counts and unique user contributions are summarized in **Table 6.**

The 17 clusters can be grouped into four functional categories based on their spatial association with recognizable heritage features and visitor-use spaces. The main temple core accounts for eight clusters concentrated around the Shiva, Vishnu, and Brahma structures and the area immediately east of Shiva, totaling approximately 1,237 clustered photographs or 57.5% of all clustered records. The Shiva Temple area contains the largest number of distinct clusters, consistent with its architectural prominence as the tallest structure in the complex. Multiple clusters along the eastern approach correspond to a sequence of progressively closer viewing positions along the primary entrance corridor, from the first unobstructed temple silhouette to carved relief panels at close range. This corridor carries the highest intra-site photographic density and may be prioritized for follow-up field observation to assess whether photographic concentration corresponds to visitor flow, interpretation, or conservation-management concerns (Leask, 2016; Prasidya et al., 2025). Brahma and Vishnu temple clusters are more compact, reflecting differences in architectural scale and visitor access relative to the Shiva complex.

**Table 5**. HDBSCAN parameter sweep results for the Candi Prambanan analytical zone.

| No | Min Cluster Size | Min Points | Clusters | Total Points | Clustered | Noise | Noise Ratio | Silhouette | DBI |
|---|---|---|---|---|---|---|---|---|---|
| 1 | 10 | 3 | 158 | 4,812 | 3,805 | 1,007 | 0.209 | 0.666 | 0.556 |
| 2 | 10 | 5 | 143 | 4,812 | 3,493 | 1,319 | 0.274 | 0.722 | 0.468 |
| 3 | 20 | 5 | 68 | 4,812 | 3,319 | 1,493 | 0.31 | 0.637 | 0.51 |
| 4 | 30 | 10 | 43 | 4,812 | 2,679 | 2,133 | 0.443 | 0.712 | 0.444 |
| 5 | 50 | 10 | 24 | 4,812 | 2,323 | 2,489 | 0.517 | 0.684 | 0.428 |
| 6 | 50 | 15 | 22 | 4,812 | 2,193 | 2,619 | 0.544 | 0.706 | 0.356 |
| 7 | 60 | 10 | 20 | 4,812 | 2,352 | 2,460 | 0.511 | 0.651 | 0.456 |
| **8** | **60** | **15** | **17** | **4,812** | **2,151** | **2,661** | **0.553** | **0.682** | **0.394** |

Note: Bold row indicates the selected configuration. The 60/15 configuration was selected for parsimony and interpretability, not because it optimizes every metric: 50/15 achieves a lower DBI (0.356), and 10/5 achieves a higher Silhouette (0.722). Silhouette and DBI were calculated on clustered observations only.

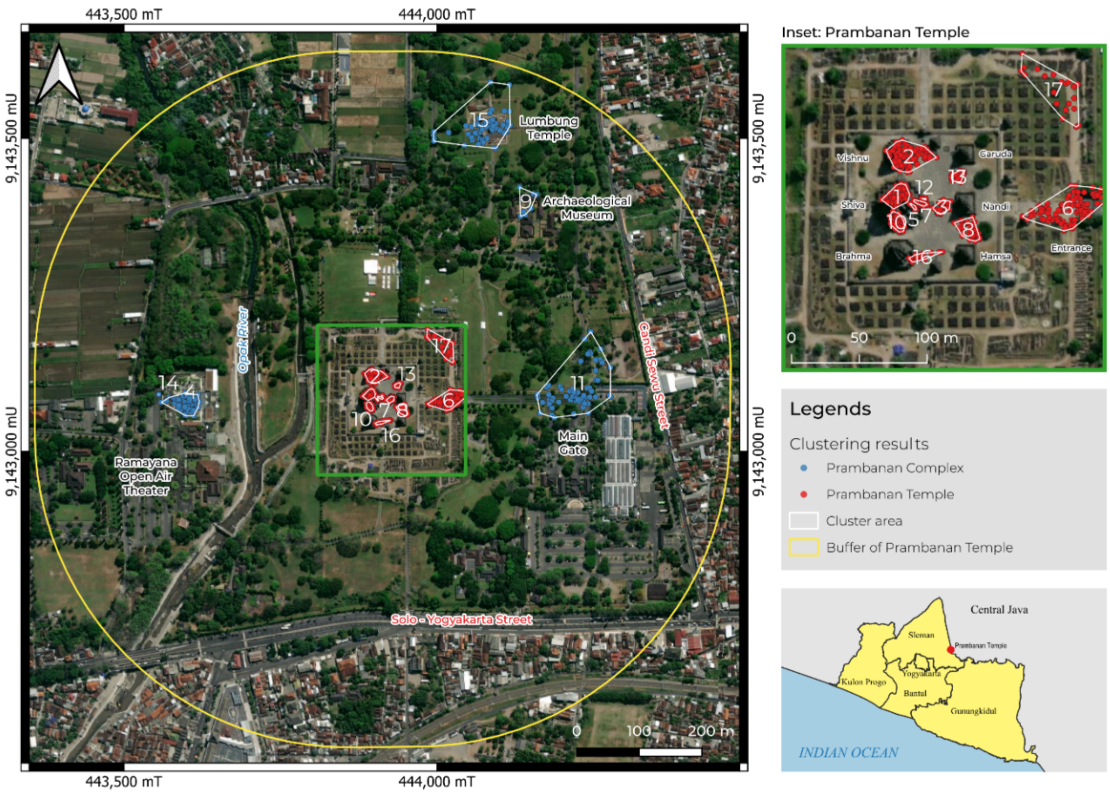


**Figure 7**. HDBSCAN clustering result for the Candi Prambanan analytical zone (Source: Authors' analysis, 2026)

The eastern pervira and small temple grouping comprises four clusters: Eastern Pervira, the area between Nandi and Hamsa temples, the Garuda-Nandi transitional space, and Northeast Pervira. These clusters are spatially more compact than those in the main core, suggesting more localized photographic concentration tied to specific architectural features or framing positions in the eastern precinct.

Two visitor facility clusters appear: the Main Entrance (92 photographs, 50 unique users) and the Archaeological Museum (114 photographs, 5 unique users). The entrance cluster reflects broadly shared photographic activity at arrival and departure sequences common to major heritage sites (Lew & McKercher, 2006). The Archaeological Museum cluster warrants caution: its moderate photograph count rests on only 5 contributors, so its spatial density may reflect concentrated uploads from a small number of users rather than distributed photographic attention across the facility.

Peripheral heritage nodes include three clusters at the Ramayana Open Air Theater and Candi Lumbung. Cluster 4 at the theater draws 184 photographs from 18 unique users, indicating multi-user photographic activity at this performing-arts venue. Cluster 14, also at the theater, concentrates 66 photographs from a single user and should not be treated as evidence of broadly shared photographic interest. The Candi Lumbung cluster comprises 64 photographs from 19 unique users, indicating modest but multi-user photographic activity at this secondary heritage structure within the Candi Prambanan analytical zone.

The 2,661 noise observations (55.3%) indicate photographs that did not meet the density criteria under the selected HDBSCAN parameters. They may include dispersed photographic activity across the complex and should not be interpreted as direct evidence of any particular spatial pattern. Clusters at peripheral and facility locations require additional field observation before their spatial significance can be assessed.

**Table 6**. Per-cluster statistics for the selected HDBSCAN configuration (min cluster size = 60, min points = 15) within the Candi Prambanan analytical zone.

| Cluster ID | Photographs (n) | % of Total (4,812) | % of Clustered (2,151) | Unique Users (n) | Dominant Location | Functional Category |
|---|---|---|---|---|---|---|
| 1 | 279 | 5.8 | 12.97 | 47 | Shiva Temple | Main temple core |
| 2 | 203 | 4.22 | 9.44 | 36 | Vishnu Temple | Main temple core |
| 3 | 201 | 4.18 | 9.34 | 20 | East of Shiva Temple | Main temple core |
| 4 | 184 | 3.82 | 8.55 | 18 | Ramayana Open Air Theater | Peripheral heritage node |
| 5 | 162 | 3.37 | 7.53 | 45 | Shiva Temple | Main temple core |
| 6 | 137 | 2.85 | 6.37 | 57 | Eastern Pervira | Eastern pervira and small temples |
| 7 | 134 | 2.78 | 6.23 | 16 | Shiva Temple | Main temple core |
| 8 | 120 | 2.49 | 5.58 | 34 | Between Nandi and Hamsa Temples | Eastern pervira and small temples |
| 9 | 114 | 2.37 | 5.30 | 5 | Archaeological Museum | Visitor facility and circulation |
| 10 | 113 | 2.35 | 5.25 | 24 | Shiva Temple | Main temple core |
| 11 | 92 | 1.91 | 4.28 | 50 | Main Entrance | Visitor facility and circulation |
| 12 | 81 | 1.68 | 3.77 | 4 | Shiva Temple | Main temple core |
| 13 | 75 | 1.56 | 3.49 | 11 | Between Garuda and Nandi Temples | Eastern pervira and small temples |
| 14 | 66 | 1.37 | 3.07 | 1 | Ramayana Open Air Theater | Peripheral heritage node* |
| 15 | 64 | 1.33 | 2.98 | 19 | Candi Lumbung | Peripheral heritage node |
| 16 | 64 | 1.33 | 2.98 | 14 | Brahma Temple | Main temple core |
| 17 | 62 | 1.29 | 2.88 | 19 | Northeast Pervira | Eastern pervira and small temples |
| Clustered total | 2,151 | 44.7 | 100 | - | - | - |
| Noise (Cluster 0) | 2,661 | 55.3 | - | - | - | - |

Note: Unique user counts indicate the number of distinct Flickr contributors per cluster. Clusters with high photograph counts but few unique users warrant cautious interpretation. Cluster 14 (66 photographs, 1 user) likely reflects individual upload behavior rather than shared photographic attention. Percentages of clustered photographs use 2,151 as the denominator.

**Implications for Heritage Tourism Management**

Across the four methods, Flickr photographic activity in Sleman's temple heritage landscape concentrates in the Candi Prambanan analytical zone, organizes around identifiable spatial nodes within that zone, and displays endpoint-sensitive temporal variation interpreted in relation to platform dynamics and external disruptions. The findings identify candidate locations for field-based monitoring at three spatial scales, with the caveat that all management inferences require field validation before being treated as confirmed evidence of visitor pressure or site deterioration.

At the site level, the main temple core and eastern circulation corridor show the strongest photographic concentrations across static and density-based analyses. Both are candidates for follow-up field observation on visitor flow, interpretation needs, and conservation-management concerns, ideally combined with site-management knowledge and local operational experience.

At the complex level, EHSA results do not support the interpretation that any location within the Candi Prambanan analytical zone is experiencing sustained or intensifying photographic growth. Oscillating Hot Spots indicate temporal instability rather than directional change. Candi Lumbung and the Ramayana Open Air Theater attract multi-user photographic activity but at volumes modest relative to the main temple core. Real-time monitoring across multiple social media platforms could complement Flickr-based analysis and provide more temporally current signals (Mariani & Baggio, 2022; Tenkanen et al., 2017).

At the landscape level, sparse Flickr records at smaller sites reflect the limits of platform-dependent data, not the absence of management needs. Future work could examine whether improved accessibility, interpretation, or promotion at secondary sites shifts photographic attention, but such questions require evaluation through direct visitor counts and management records.

The contrast between OHSA and EHSA is central to the study's contribution. Static hot spot analysis identifies the Candi Prambanan analytical zone as the dominant spatial concentration, whereas EHSA classifies this concentration as predominantly oscillating rather than persistent or intensifying within the selected 2005–2025 temporal window. Static social-media hot spots may indicate photographic prominence without demonstrating sustained growth, crowding, or physical pressure, and single-period hot spot maps risk overstating the stability of apparent concentrations in heritage contexts where platform activity and external disruptions reshape temporal patterns (Bettaieb & Wakabayashi, 2023; Morckel & Durst, 2023; Purwanto et al., 2021). HDBSCAN adds a third layer by resolving intra-site photographic nodes invisible at the landscape scale but relevant for site-level monitoring planning.

The combined results also show that statistical significance, visual prominence, and management relevance do not always align. Candi Lumbung appears as a relative cold spot in OHSA but remains identifiable as a modest HDBSCAN photographic node, while the main gate area of Ratu Boko is visually prominent but does not form a statistically significant hot spot under any tested OHSA configuration. Flickr-based hot spot outputs are therefore best read as indicators of relative photographic concentration, not as direct measures of visitor value, scenic importance, or management urgency.

The narrowing of statistically interpretable spatiotemporal results to the Candi Prambanan analytical zone marks a practical boundary of Flickr-based heritage analysis. Quadrat density and OHSA can describe and test spatial concentration where the available photographs produce sufficient local contrast, whereas EHSA requires records to be distributed repeatedly across both spatial bins and annual time steps. In this study, statistically classified EHSA patterns emerged only at Prambanan. The absence of classified patterns at the smaller sites should therefore be interpreted as a limitation of the available spatial and temporal distribution of Flickr records, not as evidence of temporal stability or inactivity.

## CONCLUSION

This study analyzed 5,858 geotagged Flickr photographs located within analytical buffer zones for 13 temple-related heritage locations in Sleman Regency, covering records dated between 2005 and 2025, using quadrat density analysis, OHSA, EHSA, and HDBSCAN clustering. Flickr photographs are treated throughout as indicators of photographic activity and spatial attention within defined analytical zones.

Photographic activity concentrates in the Candi Prambanan analytical zone (82.14% of retained photographs), though area-adjusted density qualifies this picture. Candi Ijo produces approximately 114 photographs per hectare within its 80 m buffer, compared with approximately 61 photographs per hectare in the Candi Prambanan analytical zone, showing that smaller sites can generate locally intense photographic activity despite lower absolute counts. Secondary sites are sparsely represented, reflecting the uneven visibility of smaller heritage locations in Flickr data.

Within the Candi Prambanan analytical zone, EHSA identifies 372 locations with significant spatiotemporal patterns, comprising 365 Oscillating Hot Spots and 7 Sporadic Hot Spots across 21 annual time steps. No locations carry persistent, consecutive, or intensifying classifications. Because both reported categories require statistically significant hot spot status in the final time step and the 2025 interval contains only 94 photographs, the resulting classifications are conditional on the selected temporal window. The broader temporal variation is discussed in the context of declining Flickr activity after the mid-2010s and disruption during the COVID-19 period, rather than as evidence of directional change in photographic concentration.

HDBSCAN identifies 17 clusters within the Candi Prambanan analytical zone corresponding to recognizable heritage features and visitor-use spaces, with the Shiva Temple eastern approach forming the dominant intra-site photographic node. User-level diagnostics confirm that some clusters rest on contributions from many unique users while others reflect a small number of prolific uploaders, a distinction relevant when interpreting cluster density as photographic concentration rather than collective photographic interest.

The combination of static, spatiotemporal, and density-based methods shows that single-period hot spot maps can misrepresent the temporal stability of photographic concentration in heritage landscapes. The main temple core, eastern circulation corridor, main entrance, Archaeological Museum, Candi Lumbung, and Ramayana Open Air Theater are candidate locations for field-based observation, though photograph density does not substitute for direct visitor counts, conservation assessment, or site-condition records.

Platform bias toward internationally connected users, declining Flickr activity after the mid-2010s, and buffer-size effects on raw counts remain the principal limitations. Integrating Instagram, Google Maps reviews, and mobile positioning data could improve representativeness and temporal coverage in future research. Applying the framework to other Indonesian heritage landscapes would test its generalizability across multi-site heritage systems.

## CONFLICTS OF INTEREST

The authors declare that they have no known competing financial interests or personal relationships that could have appeared to influence the work reported in this paper.

## AUTHOR CONTRIBUTION

Conceptualization and methodology: **T.W.W.** and **S.H.M.B.**; investigation: **B.S.** and **T.H.P.**; writing original draft preparation: **T.W.W.** and **B.S.**; writing review and editing: **T.W.W.** and **S.H.M.B.**; visualization: **T.W.W.** and **B.K.** All authors have read and agreed to the published version of the manuscript.

## FUNDING

This research was supported by the 2025 Independent Lecturer Grants, Faculty of Geography, UGM, with the Grant Number 109/UN1/GE/KPT/2025.

## ACKNOWLEDGMENT

The authors are grateful to the anonymous reviewers for their valuable feedback on the improvement of this manuscript.

## DATA AVAILABILITY

The Flickr metadata used in this study were obtained from publicly accessible records through the Flickr API. Raw user-level metadata are not redistributed due to platform terms and privacy considerations. The API endpoint, retrieval date, search extent, buffer definitions, and aggregated analytical summaries are reported in the manuscript. Aggregated tables and derived outputs are available from the corresponding author upon reasonable request.

## REFERENCE LIST

Adie, B. A., Falk, M., & Savioli, M. (2020). Overtourism as a perceived threat to cultural heritage in Europe. Current Issues in Tourism, 23(14), 1737–1741. https://doi.org/10.1080/13683500.2019.1687661

Al-Saad, S. A., Jawarneh, R. N., & Aloudat, A. S. (2023). Spatiotemporal cluster analysis of reputable tourist accommodation in Greater Amman Municipality, Jordan. Journal of Hospitality and Tourism Technology, 14(4), 579–597. https://doi.org/10.1108/JHTT-03-2021-0071

Bettaieb, B., & Wakabayashi, Y. (2023). Visualising temporal changes in visitors' areas of interest using online geotagged photographs. International Journal of Cartography, 9(3), 488–506. https://doi.org/10.1080/23729333.2023.2236267

Caldas de Castro, M., & Singer, B. H. (2006). Controlling the False Discovery Rate: A New Application to Account for Multiple and Dependent Tests in Local Statistics of Spatial Association. Geographical Analysis, 38(2), 180–208. https://doi.org/10.1111/j.0016-7363.2006.00682.x

Campello, R. J. G. B., Moulavi, D., & Sander, J. (2013). Density-Based Clustering Based on Hierarchical Density Estimates. In J. Pei, V. S. Tseng, L. Cao, H. Motoda, & G. Xu (Eds.), Advances in Knowledge Discovery and Data Mining (Vol. 7819, pp. 160–172). Springer Berlin Heidelberg. https://doi.org/10.1007/978-3-642-37456-2_14

Coimbra, I., Conceição, P. S., Sousa, A. R., Alves, F. B., Tavares, D., & Breda-Vázquez, I. (2025). The management of urban World Heritage Sites: A semi-systematic literature review. Npj Heritage Science, 13(1), 610. https://doi.org/10.1038/s40494-025-01921-6

Dinas Pariwisata Daerah Istimewa Yogyakarta. (2024). Buku statistik kepariwisataan DIY 2023. Dinas Pariwisata DIY.

Domènech, A., Mohino, I., & Moya-Gómez, B. (2020). Using Flickr Geotagged Photos to Estimate Visitor Trajectories in World Heritage Cities. ISPRS International Journal of Geo-Information, 9(11), 646. https://doi.org/10.3390/ijgi9110646

Dong, W., Kang, Q., Wang, G., Zhang, B., & Liu, P. (2023). Spatiotemporal behavior pattern differentiation and preference identification of tourists from the perspective of ecotourism destination based on the tourism digital footprint data. PLOS ONE, 18(4), e0285192. https://doi.org/10.1371/journal.pone.0285192

ESRI. (2021, September 20). How Emerging Hot Spot Analysis works. ArcGIS Desktop Resources. https://desktop.arcgis.com/en/arcmap/latest/tools/space-time-pattern-mining-toolbox/learnmoreemerging.htm

Fast, V. (2024). GIScience I: The rise, fragmentation, and future of VGI. Progress in Human Geography, 48(6), 922–933. https://doi.org/10.1177/03091325241277834

Flickr. (2024, September 5). Flickr APIs Terms of Use. Flickr API. https://www.flickr.com/help/terms/api

García-Palomares, J. C., Gutiérrez, J., & Mínguez, C. (2015). Identification of tourist hot spots based on social networks: A comparative analysis of European metropolises using photo-sharing services and GIS. Applied Geography, 63, 408–417. https://doi.org/10.1016/j.apgeog.2015.08.002

Getis, A., & Ord, J. K. (1992). The Analysis of Spatial Association by Use of Distance Statistics. Geographical Analysis, 24(3), 189–206. https://doi.org/10.1111/j.1538-4632.1992.tb00261.x

Ghermandi, A. (2022). Geolocated social media data counts as a proxy for recreational visits in natural areas: A meta-analysis. Journal of Environmental Management, 317, 115325. https://doi.org/10.1016/j.jenvman.2022.115325

Ghermandi, A., & Sinclair, M. (2019). Passive crowdsourcing of social media in environmental research: A systematic map. Global Environmental Change, 55, 36–47. https://doi.org/10.1016/j.gloenvcha.2019.02.003

Haklay, M. (2013). Citizen Science and Volunteered Geographic Information: Overview and Typology of Participation. In D. Sui, S. Elwood, & M. Goodchild (Eds.), Crowdsourcing Geographic Knowledge: Volunteered Geographic Information (VGI) in Theory and Practice (pp. 105–122). Springer Netherlands. https://doi.org/10.1007/978-94-007-4587-2_7

Hollenstein, L., & Purves, R. (2010). Exploring place through user-generated content: Using Flickr to describe city cores. Journal of Spatial Information Science, (1), 21–48. https://doi.org/10.5311/JOSIS.2010.1.3

Jenks, G. F. (1967). The data model concept in statistical mapping. International Yearbook of Cartography, 7, 186–190.

Karayazi, S. S., Dane, G., & Arentze, T. (2022). An Exploration of Interactions Between Urban Heritages and Tourist's Digital Footprint: Network and Textual Analysis via Geotagged Flickr Data in Amsterdam. ISPRS Annals of the Photogrammetry, Remote Sensing and Spatial Information Sciences, X-4/W3-2022, 105–112. https://doi.org/10.5194/isprs-annals-X-4-W3-2022-105-2022

Kim, S., Lee, J., & Kim, Y. (2024). Evaluation of Urban Traditional Temples Using Cultural Tourism Potential. Sustainability, 16(15), 6375. https://doi.org/10.3390/su16156375

Leask, A. (2016). Visitor attraction management: A critical review of research 2009–2014. Tourism Management, 57, 334–361. https://doi.org/10.1016/j.tourman.2016.06.015

Lee, J. Y., & Tsou, M.-H. (2018). Mapping Spatiotemporal Tourist Behaviors and Hotspots Through Location-Based Photo-Sharing Service (Flickr) Data. In P. Kiefer, H. Huang, N. Van de Weghe, & M. Raubal (Eds.), Progress in Location Based Services 2018 (pp. 315–334). Springer International Publishing.

Leppämäki, T., Heikinheimo, V., Eklund, J., Hausmann, A., & Toivonen, T. (2025). The rise and fall of the social media platform Flickr: Implications for nature recreation research. Journal of Outdoor Recreation and Tourism, 50, 100880. https://doi.org/10.1016/j.jort.2025.100880

Lew, A., & McKercher, B. (2006). Modeling Tourist Movements. Annals of Tourism Research, 33(2), 403–423. https://doi.org/10.1016/j.annals.2005.12.002

López-Guzmán, T., Sánchez-Cañizares, S. M., & Pavón, V. (2011). Community-based tourism in developing countries: A case study. Tourismos, 6(1), 69–84.

Mancini, F., Coghill, G. M., & Lusseau, D. (2018). Using social media to quantify spatial and temporal dynamics of nature-based recreational activities.

PLOS ONE, 13(7), e0200565. https://doi.org/10.1371/journal.pone.0200565

Mariani, M., & Baggio, R. (2022). Big data and analytics in hospitality and tourism: A systematic literature review. International Journal of Contemporary Hospitality Management, 34(1), 231–278. https://doi.org/10.1108/IJCHM-03-2021-0301

Martins, M., & Santos, A. (2024). Exploring the potential of Flickr User-Generated Content for Tourism Research: Insights from Portugal. European Journal of Tourism, Hospitality and Recreation, 14(2), 258–272. https://doi.org/10.2478/ejthr-2024-0019

McInnes, L., Healy, J., & Astels, S. (2017). hdbscan: Hierarchical density based clustering. The Journal of Open Source Software, 2(11), 205. https://doi.org/10.21105/joss.00205

McKercher, B., & Koh, E. (2017). Do attractions "attract" tourists? The case of Singapore. International Journal of Tourism Research, 19(6), 661–671. https://doi.org/10.1002/jtr.2138

Meng, L., Du, Z., Jia, Z., & Cao, L. (2025). Spatial Mechanisms and Coupling Coordination of Cultural Heritage and Tourism Along the Jinzhong Segment of the Great Tea Road. Heritage, 9(1), 7. https://doi.org/10.3390/heritage9010007

Morckel, V., & Durst, N. (2023). Using Emerging Hot Spot Analysis to Explore Spatiotemporal Patterns of Housing Vacancy in Ohio Metropolitan Statistical Areas. Urban Affairs Review, 59(1), 309–328. https://doi.org/10.1177/10780874211065014

Payntar, N. D., Hsiao, W.-L., Covey, R. A., & Grauman, K. (2021). Learning Patterns of Tourist Movement and Photography from Geotagged Photos at Archaeological Heritage Sites in Cuzco, Peru. Tourism Management, 82, 104165. https://doi.org/10.1016/j.tourman.2020.104165

Prasidya, A. S., Gumilar, I., Meilano, I., Ikaputra, I., Muryamto, R., & Arrofiqoh, E. N. (2025). Three-Dimensional Digital Documentation for the Conservation of the Prambanan Temple Cluster Using Guided Multi-Sensor Techniques. Heritage, 8(1), 32. https://doi.org/10.3390/heritage8010032

Purwanto, P., Utaya, S., Handoyo, B., Bachri, S., Astuti, I. S., Utomo, K. S. B., & Aldianto, Y. E. (2021). Spatiotemporal Analysis of COVID-19 Spread with Emerging Hotspot Analysis and Space–Time Cube Models in East Java, Indonesia. ISPRS International Journal of Geo-Information, 10(3), 133. https://doi.org/10.3390/ijgi10030133

Sedmak, G., Paliska, D., & Brezovec, A. (2023). Data Mining of Visitors' Spatial Movement Patterns Using Flickr Geotagged Photos: The Case of Dispersed Plečnik's Architectural Heritage in Ljubljana. Academica Turistica, 49–62. https://doi.org/10.26493/2335-4194.16.49-62

Sigurbjörnsson, B., & Van Zwol, R. (2008). Flickr tag recommendation based on collective knowledge. Proceedings of the 17th International Conference on World Wide Web, 327–336. https://doi.org/10.1145/1367497.1367542

Teles Da Mota, V., & Pickering, C. (2020). Using social media to assess nature-based tourism: Current research and future trends. Journal of Outdoor Recreation and Tourism, 30, 100295. https://doi.org/10.1016/j.jort.2020.100295

Tenkanen, H., Di Minin, E., Heikinheimo, V., Hausmann, A., Herbst, M., Kajala, L., & Toivonen, T. (2017). Instagram, Flickr, or Twitter: Assessing the usability of social media data for visitor monitoring in protected areas. Scientific Reports, 7(1), 17615. https://doi.org/10.1038/s41598-017-18007-4

Timothy, D. J., & Boyd, S. W. (2003). Heritage Tourism. Prentice Hall.

UNESCO. (1991). Prambanan Temple Compounds. Prambanan Temple Compounds - UNESCO World Heritage Centre. https://whc.unesco.org/en/list/642/

Urry, J., & Larsen, J. (2011). The Tourist Gaze 3.0. SAGE Publications Ltd. https://doi.org/10.4135/9781446251904

Wibowo, T. W., Rofi'i, A., & Sulistyaningrum, N. A. (2019). Density analysis of Flickr data as a proxy to reveal the intensity of tourism activity in Borobudur. In S. B. Wibowo, A. B. Rimba, A. A. Aziz, S. Phinn, J. T. Sri Sumantyo, H. Widyasamratri, & S. Arjasakusuma (Eds.), Sixth Geoinformation Science Symposium (p. 39). SPIE. https://doi.org/10.1117/12.2549040

Wicaksono, A., Farda, N. M., Khakhim, N., & Wibowo, T. W. (2021). Flickr Photos Analysis for Beach Tourism Management in Bantul Regency, Indonesia: Popularity and Tourist Attractions. Forum Geografi, 35(1). https://doi.org/10.23917/forgeo.v35i1.13007

Widjanarko, H., Utomo, H. S., & Suratna. (2023). Unlocking Success for Cultural Tourism Villages in Yogyakarta: Insights from Wukirsari Village. Advances in Social Science, Education and Humanities Research, 505–511. https://doi.org/10.2991/978-2-38476-048-0_53

Wilkins, E. J., Wood, S. A., & Smith, J. W. (2021). Uses and Limitations of Social Media to Inform Visitor Use Management in Parks and Protected Areas: A Systematic Review. Environmental Management, 67(1), 120–132. https://doi.org/10.1007/s00267-020-01373-7

Zhang, G., & Zhu, A.-X. (2018). The representativeness and spatial bias of volunteered geographic information: A review. Annals of GIS, 24(3), 151–162. https://doi.org/10.1080/19475683.2018.1501607